JETIR.ORG ISSN: 2349-5162 | ESTD Year : 2014 | Monthly Issue
JOURNAL OF EMERGING TECHNOLOGIES AND INNOVATIVE RESEARCH (JETIR)
An International Scholarly Open Access, Peer-reviewed, Refereed Journal

Review and Comparison of Isolated DC-DC Converters for Electric Vehicle Applications

[1]Smitha Joseph

[1]Lecturer in Electrical and Electronics Engineering,
[1]Department of Electrical and Electronics Engineering,
[1]Government Polytechnic College, Kalamassery, Kerala, India

Abstract : The rapid proliferation of electric vehicles (EVs) has created unprecedented demand for high-efficiency, high-power-density isolated DC-DC converters for both on-board and off-board charging applications. This comprehensive review examines the current state-of-the-art in isolated DC-DC converter topologies for EV charging, including Dual Active Bridge (DAB), LLC resonant, CLLC bidirectional resonant, and Phase-Shifted Full-Bridge (PSFB) converters. The paper presents a systematic comparison of these topologies based on efficiency, power density, control complexity, and suitability for Vehicle-to-Grid (V2G) applications. Additionally, the impact of Wide Bandgap (WBG) semiconductors, specifically Silicon Carbide (SiC) and Gallium Nitride (GaN), on converter performance is analyzed. Through examination of 30 peer-reviewed publications from 2020-2023, this review identifies optimal topology-application pairings, highlights emerging trends including modular architectures for ultra-fast charging (350 kW+), and discusses research gaps requiring further investigation. The findings indicate that SiC-based DAB and CLLC converters achieve efficiencies exceeding 98% with power densities above 2 kW/L, making them particularly suitable for next-generation EV charging infrastructure.

IndexTerms **- DC-DC converters, electric vehicles, dual active bridge, LLC resonant, CLLC, phase-shifted full-bridge, SiC MOSFET, GaN HEMT, V2G, fast charging**

I. INTRODUCTION

The global transition toward sustainable transportation has positioned electric vehicles as a cornerstone of decarbonization efforts, with the International Energy Agency projecting over 300 million EVs on roads by 2030 [1]. This exponential growth has intensified the demand for efficient, reliable, and high-power charging infrastructure. At the heart of every EV charging system lies the DC-DC converter, which plays a critical role in managing power flow between the grid, charging station, and vehicle battery [2]. Isolated DC-DC converters are preferred for EV applications due to their inherent safety benefits, providing galvanic isolation between the high-voltage battery pack (typically 300-800V) and external systems [3]. The isolation requirement is particularly important for on-board chargers (OBCs) that connect directly to the AC grid and for DC fast charging stations where multiple vehicles may charge simultaneously [4]. Furthermore, the emergence of Vehicle-to-Grid (V2G) technology, enabling bidirectional power flow between EVs and the electrical grid, has added new requirements for converter design, necessitating efficient operation in both charging and discharging modes [5]. The evolution of power semiconductor technology has fundamentally transformed converter design possibilities. Wide Bandgap (WBG) semiconductors, particularly Silicon Carbide (SiC) MOSFETs and Gallium Nitride (GaN) High Electron Mobility Transistors (HEMTs), offer superior switching characteristics compared to traditional Silicon (Si) devices [6]. SiC devices enable efficient operation at switching frequencies exceeding 100 kHz with voltage ratings up to 1700V, making them ideal for high-power EV charging applications [7]. GaN HEMTs, with their exceptional switching speeds and low gate charge, are increasingly adopted in lower-power OBCs where switching frequencies in the megahertz range can significantly reduce passive component sizes [8].

This paper provides a comprehensive review of isolated DC-DC converter topologies for EV applications, addressing five key objectives. First, it presents a systematic classification of isolated DC-DC converter topologies based on power flow capability and switching characteristics. Second, it provides detailed analysis of dominant topologies including DAB, LLC, CLLC, and PSFB converters with their operating principles and design considerations. Third, it offers a quantitative comparison of efficiency and power density achievements reported in recent literature, synthesizing data from 30 peer-reviewed publications. Fourth, it assesses the impact of WBG semiconductor technology on converter performance, comparing SiC and GaN devices with traditional silicon solutions. Finally, it identifies research gaps and proposes future research directions to guide ongoing development efforts.

The remainder of this paper is organized as follows. Section II presents the classification of isolated DC-DC topologies based on power flow direction, switching mechanism, and resonant characteristics. Section III provides detailed analysis of each major topology, including operating principles, modulation strategies, and recent research advances. Section IV discusses semiconductor technology considerations, comparing Silicon, SiC, and GaN devices for EV charging applications. Section V presents comparative analysis and discussion of efficiency and power density achievements. Section VI covers emerging trends and applications including

ultra-fast charging, 800V systems, wireless power transfer, and V2G infrastructure. Section VII identifies research gaps, and Section VIII concludes with a summary of key findings and recommendations.

II. Classification of Isolated DC-DC Converter Topologies

Isolated DC-DC converters for EV applications can be classified based on multiple criteria including power flow direction, switching mechanism, and resonant characteristics. Figure 1 presents a comprehensive taxonomy of the converter topologies discussed in this review.

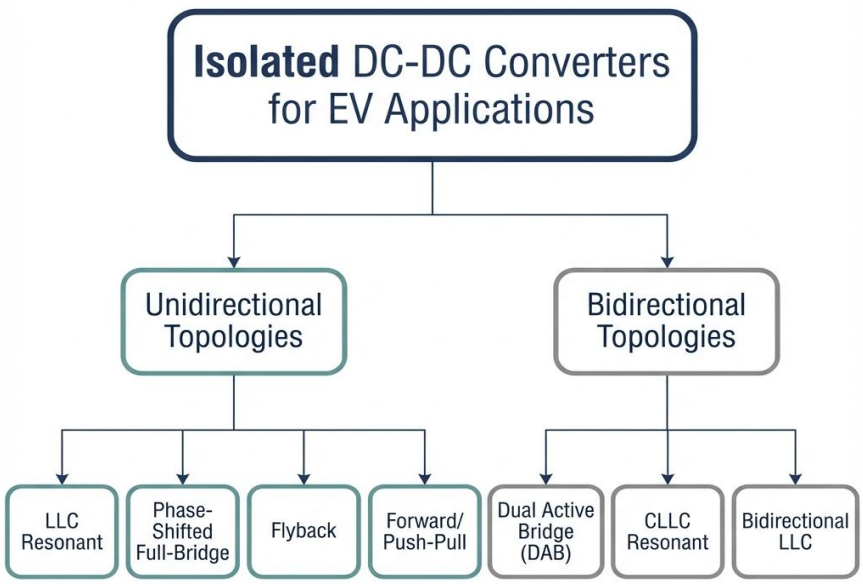

Figure 1: Hierarchical classification of isolated DC-DC converter topologies for electric vehicle applications, categorized by power flow direction (unidirectional vs. bidirectional) and switching characteristics.

2.1 Classification by Power Flow Direction

2.1.1 Unidirectional converters

These converters transfer power in a single direction, typically from the grid or charging station to the EV battery. These topologies are simpler in design and control, making them suitable for applications where V2G functionality is not required [9]. Common unidirectional topologies include LLC resonant converters, Phase-Shifted Full-Bridge (PSFB) converters, and flyback converters for auxiliary power applications [10].

2.1.2 Bidirectional converters

These converters enable power flow in both directions, supporting Grid-to-Vehicle (G2V) charging and Vehicle-to-Grid (V2G) discharging. The bidirectional capability is increasingly important as V2G technology matures, enabling EVs to provide grid services such as frequency regulation, peak shaving, and backup power [11]. The Dual Active Bridge (DAB) and CLLC resonant converters are the dominant bidirectional topologies in current research and commercial development [12].

2.2 Classification by Switching Mechanism

2.2.1 Hard-switching converters

Hard-switching converters operate with significant overlap between switch current and voltage during transitions, resulting in switching losses that increase with frequency. While simpler to design, hard-switching converters are generally limited to lower switching frequencies (typically below 50 kHz) to maintain acceptable efficiency [13].

2.2.2 Soft-switching converters

Soft-switching converters achieve Zero Voltage Switching (ZVS) and/or Zero Current Switching (ZCS), minimizing switching losses and enabling higher operating frequencies [14]. The Phase-Shifted Full-Bridge converter achieves ZVS through phase-shift control, while resonant topologies (LLC, CLLC) inherently provide soft-switching through their resonant tank characteristics [15]. Soft-switching is essential for high-efficiency operation, particularly when utilizing WBG semiconductors at frequencies above 100 kHz [16].

2.3 Classification by Resonant Characteristics

2.3.1 Non-resonant converters

Non-resonant converters such as the basic DAB and PSFB rely on inductive energy storage and PWM or phase-shift modulation for voltage regulation. These topologies offer straightforward control but may suffer from circulating currents under light load conditions [17].

2.3.2 Resonant converters

Resonant converters incorporate LC tank circuits that enable soft-switching operation and sinusoidal current waveforms. The LLC converter uses a series-parallel resonant tank, while the CLLC topology extends this concept with symmetric resonant tanks on both primary and secondary sides for bidirectional operation [18]. Resonant converters typically achieve the highest efficiencies but require careful design of the resonant tank parameters to maintain soft-switching across the operating range [19].

The key characteristics of major isolated DC-DC converter topologies for EV applications are summarized in the table below.

Table I: Summary of Isolated DC-DC Converter Topologies for EV Applications

Topology	Power Flow	Soft-Switching	Typical Efficiency	Power Range	Primary Application
DAB	Bidirectional	ZVS	94-98%	1-100 kW	On-Board Charger, Vehicle-to-Grid
LLC	Unidirectional	ZVS	95-98%	1-22 kW	On-Board Charger
CLLC	Bidirectional	ZVS	97-98.5%	3-11 kW	On-Board Charger, Vehicle-to-Grid
PSFB	Unidirectional	ZVS	93-96%	1-10 kW	On-Board Charger, Auxiliary Power Module
Flyback	Unidirectional	Hard/Soft	85-92%	10-200 W	Auxiliary Power Module
Forward	Unidirectional	Hard	88-93%	100-1000 W	Auxiliary Power Module

III. Detailed Analysis of Major Topologies

This section provides in-depth analysis of the dominant isolated DC-DC converter topologies for EV charging applications, including operating principles, modulation strategies, design considerations, and recent research advances.

3.1 Dual Active Bridge (DAB) Converter

The Dual Active Bridge converter, first introduced by De Doncker et al. in 1991 [33], has become one of the most extensively studied topologies for bidirectional EV charging due to its symmetrical structure, inherent soft-switching capability, and excellent power density [12]. Figure 3 shows the circuit schematic of a typical DAB converter.

3.1.1 Operating Principle

A dual active bridge (DAB) converter consists of two full-bridge converters connected through a high-frequency transformer. Power transfer is controlled by adjusting the phase shift (φ) between the primary and secondary bridge switching signals [34]. For Single Phase Shift (SPS) modulation, the power transfer relationship is:

$$P = (n \times Vin \times Vout / (2 \times pi \times fs \times L)) \times \varphi \times (1 - |\varphi|/pi),$$

where n is the transformer turns ratio, Vin and Vout are the input and output voltages, fs is the switching frequency, L is the equivalent series inductance, and φ is the phase shift angle [35].

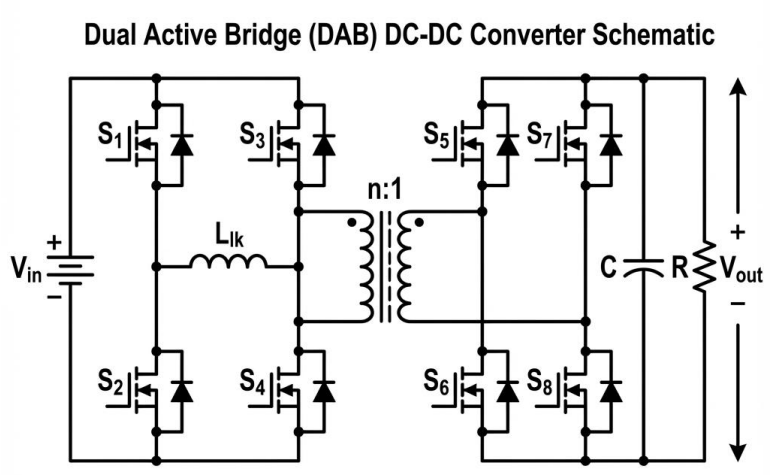

Figure 3: Circuit schematic of the Dual Active Bridge (DAB) isolated DC-DC converter showing primary-side full-bridge (S1-S4), high-frequency transformer with leakage inductance Llk, and secondary-side full-bridge (S5-S8).

3.1.2 Modulation Strategies

SPS modulation is the simplest approach, but it can produce high circulating currents and lose zero-voltage switching (ZVS) under light load or when the voltage conversion ratio deviates significantly from unity [36]. Dual Phase Shift (DPS) introduces a secondary phase shift within one bridge; Zhao et al. [37] showed it can reduce RMS current stress by up to 30% while maintaining ZVS across a wider operating range. Triple Phase Shift (TPS) uses three independent phase shifts to optimize multiple objectives; Tang et al. [38] proposed an AI-based Hybrid Extended Phase Shift (HEPS) method that achieved 97.1% peak efficiency with full-range ZVS on a 1 kW prototype. Extended Phase Shift (EPS) refinements also address practical timing effects; Jin et al. [39] developed improved triple-phase-shift control that considers dead time, achieving all-switch ZVS while minimizing current stress.

3.1.3 Design Considerations

Krismer and Kolar [40] provided foundational analytical solutions for DAB optimization, including closed-form expressions for minimum-conduction-loss modulation, and later extended this work to efficient ZVS modulation that incorporates nonlinear parasitic output capacitance effects [41]. The series inductance, often combining transformer leakage inductance with an external inductor, sets the power transfer capability and must be chosen to balance operating range against circulating current magnitude [42]. The transformer turns ratio should be selected around the nominal conversion ratio to reduce RMS currents at the most frequent operating point. Dead time selection is critical for ZVS: insufficient dead time prevents full capacitor commutation, while excessive dead time increases body-diode conduction losses; the best value depends on device output capacitances and operating current.

3.1.4 Recent Research Advances

Recent DAB research for EV applications focuses on wide voltage range operation, higher power prototypes, modular scaling, and digital control. Mirtchev and Tatakis [43] developed a dual-control approach combining frequency modulation and phase-shift control to maintain efficient soft switching across a wide EV battery range of about 250 V to 450 V. High-power demonstrations report 10–40 kW DAB converters using SiC MOSFETs with efficiencies of 97–98% [44]. Modular architectures such as Input-Series Output-Parallel (ISOP) support scaling to 350 kW and beyond for ultra-fast charging [45]. Advanced control methods, including model predictive control (MPC) and sliding mode control, have been implemented on DSP/FPGA platforms to improve dynamics and enable real-time modulation optimization [46].

3.2 LLC Resonant Converter

The LLC resonant converter is widely used for unidirectional on-board chargers because it can achieve zero-voltage switching (ZVS) for the primary switches and zero-current switching (ZCS) for the secondary diodes over a wide load range [18]. The name comes from its resonant tank, which includes a series resonant inductor Lr, a magnetizing inductance Lm, and a series resonant capacitor Cr.

3.2.1 Operating Principle

LLC operation is commonly described in frequency regions defined by the switching frequency (fs) relative to two resonant frequencies: the series resonant frequency fr and the parallel resonant frequency fp. These are given by fr = 1 / (2 × pi × sqrt(Lr × Cr)) and fp = 1 / (2 × pi × sqrt((Lr + Lm) × Cr)). Operating above fr helps ensure ZVS for the primary switches, while operating near fr tends to maximize efficiency by reducing circulating current [47]. The voltage gain shape depends strongly on the inductance ratio Ln = Lm / Lr and the quality factor Q = sqrt(Lr / Cr) / Req, where Req is the equivalent load resistance reflected to the resonant tank [48].

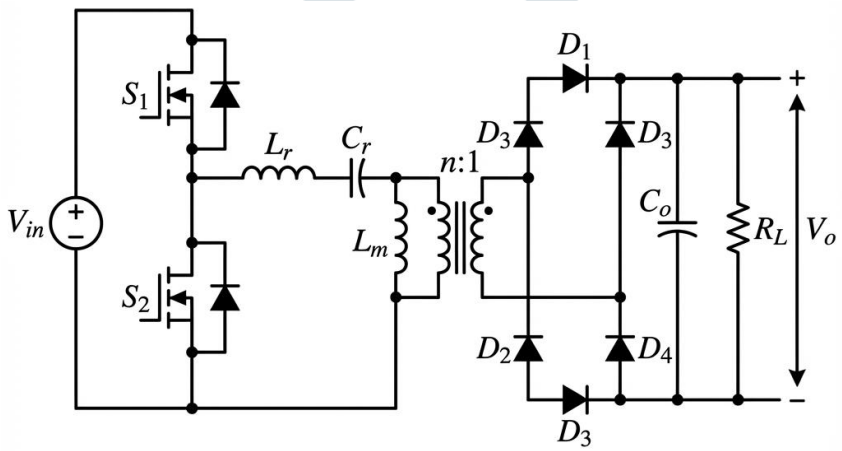

Figure 4: LLC resonant converter showing half-bridge primary with resonant tank (Lr, Lm, Cr) and center-tapped secondary rectifier.

3.2.2 Design Optimization for EV Charging

Design work for EV charging often targets constant-power and wide-operating-range requirements. Wu et al. [22] proposed a capacitor-clamped LLC approach that enables constant power charging at a fixed operating frequency, avoiding variable-frequency operation that can complicate EMI filter design, which is particularly helpful during the constant-current (CC) charging phase. Wei et al. [49] presented an automated RMS-current-based optimal design tool that co-optimizes resonant tank values, switching

frequency range, and transformer design, reducing design time and matching experimental prototypes. More broadly, multi-objective optimization typically aims to narrow the required switching-frequency span (to simplify EMI filtering), reduce resonant inductor RMS current (to lower conduction losses), maximize efficiency across the full CC–CV charging profile rather than at a single point, and preserve soft-switching under light load and voltage extremes [50].

3.2.3 Time-Weighted Average Efficiency

A key methodological shift is Time-Weighted Average Efficiency (TWAE), which optimizes efficiency over the entire charging cycle instead of maximizing peak efficiency at one operating point [51]. Because EV charging spends substantial time in both the CC phase (high current, rising voltage) and the CV phase (falling current as the battery fills), TWAE weights efficiency by time spent in each phase and has been shown to yield about 2–3% higher practical efficiency than peak-optimized designs, supported by extensive experimental validation [51].

3.2.4 High Power Density Designs

High power density LLC designs frequently use planar transformers. Reported work shows optimized planar structures can reduce transformer height by more than 50% versus conventional wound transformers while maintaining comparable power capability [52]. Techniques such as pattern arrangement and conductor-width optimization are used to reduce DC resistance and AC proximity losses, and thermal validation across −40°C to +85°C has supported suitability for automotive environments [52]. Jagadan et al. [53] also provided broader LLC design guidelines that incorporate advances in magnetic materials and semiconductors to sustain high efficiency across the full EV charging cycle.

3.3 CLLC Bidirectional Resonant Converter

The CLLC converter adapts the LLC concept to bidirectional operation by using symmetric resonant tanks on both the primary and secondary sides, enabling efficient power transfer in both directions and making it well suited to V2G-capable on-board chargers [24].

3.3.1 Topology and Operation

A typical CLLC consists of two full bridges connected through a high-frequency transformer, with resonant tanks placed on both sides. Each tank includes a series inductor (Lr1 or Lr2), the transformer magnetizing inductance, and a series capacitor (Cr1 or Cr2) [54]. The symmetry helps preserve soft-switching behavior in both grid-to-vehicle (G2V) and vehicle-to-grid (V2G) modes [25], while power flow direction is controlled through frequency modulation and the phase relationship between the two bridges.

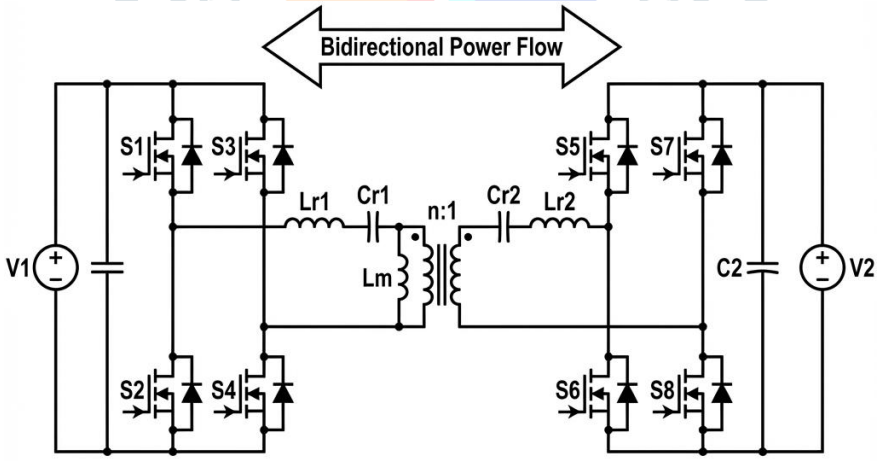

Figure 5: CLLC bidirectional resonant converter with symmetric resonant tanks on primary and secondary sides enabling bidirectional power flow for V2G applications

3.3.2 Design Methodologies

Xuan et al. [24] proposed a three-level CLLC for bidirectional EV charging in DC microgrids; by halving switch voltage stress relative to two-level designs, it can enable lower-voltage, lower-cost devices while retaining bidirectional soft switching. Zhao et al. [55] developed a design methodology for wide battery voltage operation using parameter-equivalent and time-domain models, targeting 100 V to 440 V battery variation and reporting efficiency above 96% across the range with experimental validation. Min and Ordonez [26] examined asymmetric resonant tank designs, showing that relaxing strict symmetry can improve efficiency in certain regions and potentially simplify control compared with fully symmetric CLLC designs.

3.3.3 Performance Achievements

Recent prototypes report strong results across power levels and switching frequencies. A 300 kHz, 6.6 kW SiC-based CLLC demonstrated 97.56% efficiency in forward mode and 97.75% in reverse at full load [56]. A 3.3 kW design using synchronous rectification with an integrated transformer reached 97.5% peak efficiency while reducing component count [57]. Another bidirectional resonant converter enhanced with an auxiliary LC circuit to maintain full-range soft switching achieved 98.13% efficiency in charge mode and 98.0% in discharge mode, representing high-end performance for V2G-capable converters [58].

3.3.4 Wide Voltage Range Operation

Maintaining high efficiency over a wide battery voltage span is a central challenge for CLLC converters in EV applications. One solution is hybrid modulation, where Bay et al. [59] proposed reconfigurable CLLC converters that combine pulse width modulation (PWM) and pulse frequency modulation (PFM) to extend voltage gain while keeping the switching frequency range narrow. Another approach uses reconfigurable topologies, in which half-bridge and full-bridge modes are selectively employed to handle extreme voltage ratios without requiring excessive frequency variation, thereby improving efficiency across the full battery range [59].

3.4 Phase-Shifted Full-Bridge (PSFB) Converter

The Phase-Shifted Full-Bridge (PSFB) converter is widely used in EV charging because it can achieve zero-voltage switching (ZVS) for the primary switches without additional auxiliary circuits [27]. Despite this advantage, the topology suffers from drawbacks such as duty cycle loss and a limited ZVS range under light-load conditions, which can restrict efficiency at high power.

3.4.1 Operating Principle

In a PSFB converter, power transfer is controlled using phase-shift modulation between the leading and lagging legs of a primary full bridge operating at a nominal 50% duty cycle [60]. ZVS is achieved using the energy stored in the switch output capacitances and the transformer leakage inductance. Figure 6 illustrates the PSFB topology, consisting of a full-bridge primary, a transformer with leakage inductance, and a full-bridge rectifier on the secondary side. A key limitation is duty cycle loss, which arises from the time required for current commutation between the primary and secondary; this effect grows with load current and can significantly reduce efficiency at higher power levels [61].

3.4.2 Improved PSFB Topologies

Several enhancements have been proposed to mitigate PSFB limitations. Lim et al. [27] introduced a center-tapped clamp circuit that suppresses secondary voltage oscillations, removing the need for dissipative snubber circuits. This approach also reduces conduction losses by eliminating circulating current during freewheeling intervals. Their 3.3 kW prototype maintained high efficiency over a wide output voltage range of 270 V to 420 V, matching the requirements of EV battery charging across the full

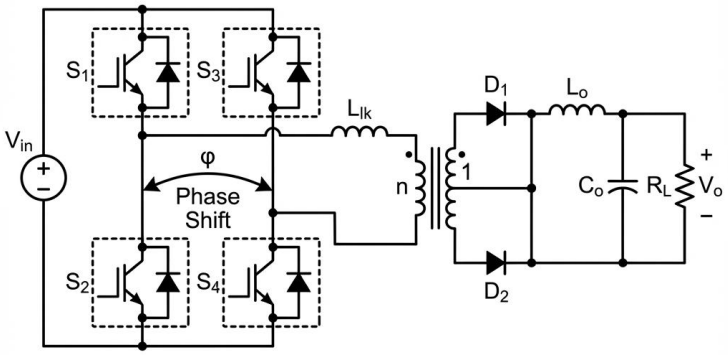

Figure 6: Phase-Shifted Full-Bridge converter with full-bridge primary, transformer with leakage inductance, and full-bridge rectifier secondary.

state-of-charge range. Telrandhe et al. [62] further provided detailed design guidelines for extending ZVS operation in PSFB-based on-board chargers, addressing component selection, dead-time optimization, and efficiency–complexity trade-offs.

3.4.3 Extended ZVS Techniques

To widen the ZVS operating region beyond that of the basic PSFB, several techniques have been reported. The coupled-inductor current-doubler method extends ZVS from light load to full load while also reducing circulating current and voltage stress on the output capacitor [63]. Auxiliary circuits, either active or passive, can supply additional commutation energy under light-load conditions where transformer current alone is insufficient for full ZVS [64]. Reconfigurable secondary architectures using series and parallel connections allow a single PSFB design to efficiently support both 400 V and emerging 800 V EV platforms, addressing the industry shift toward higher voltage systems [65].

3.4.4 Performance with Wide-Bandgap Semiconductors

Wide-bandgap devices have further improved PSFB performance. SiC-based PSFB converters have achieved peak efficiencies of about 96.5% at 200 kHz switching frequency, enabling notable reductions in size compared to lower-frequency silicon implementations [66]. Such designs are especially attractive for 12 V auxiliary battery chargers where power density is critical. GaN-based solutions have also shown strong results; for example, a 3.8 kW GaN HEMT auxiliary power module reached 96.7% peak efficiency with a power density of 3 kW/L, highlighting the suitability of GaN devices for compact auxiliary power applications [67].

IV. SEMICONDUCTOR TECHNOLOGY CONSIDERATIONS

4.1 Silicon Carbide (SiC) MOSFETs

SiC MOSFETs have revolutionized high-power EV charging applications, enabling significant improvements in efficiency and power density compared to Si-based solutions [6]. SiC offers a bandgap of 3.3 eV compared to 1.1 eV for Si, resulting in several superior material properties [68]. The higher bandgap enables a breakdown electric field approximately ten times greater than silicon, allowing thinner drift regions for equivalent voltage ratings. This translates to substantially lower on-resistance for devices rated at the same blocking voltage. SiC also exhibits thermal conductivity approximately three times higher than silicon, enabling more efficient heat extraction from the device and higher current densities. These properties allow SiC devices to operate at junction temperatures up to 175°C or higher, compared to typical 125-150°C limits for silicon devices [68].

Loncarski et al. [69] conducted a comprehensive comparison of SiC-MOSFET and Si-IGBT based interleaved DC-DC converters for EV charging, demonstrating that SiC achieves efficiencies up to 98.53% compared to approximately 95-96% for Si-IGBT at equivalent operating conditions. Ditze et al. [70] developed an 11 kW portable SiC-based charger that achieved exceptional performance metrics. The charger demonstrated a peak efficiency of 96% with sustained efficiency of 95.8% across the full battery voltage range. A power density of 2.3 kW/L was achieved, making the unit suitable for emergency and mobile charging applications where portability is essential [70].

For high-power applications, research has demonstrated the substantial benefits of SiC technology. A 20 kW SiC-based isolated DC-DC converter achieved record efficiency of 98.9%, representing the highest reported efficiency for this power class [71]. Furthermore, power densities up to 20 kW/L have been demonstrated with advanced liquid cooling thermal management systems, indicating the potential for extremely compact high-power designs [72].

4.2 Gallium Nitride (GaN) HEMTs

GaN devices offer exceptional switching speed and are particularly suited for lower-power, high-frequency applications where minimizing passive component size is critical [8]. GaN HEMTs provide several advantages derived from the material properties of gallium nitride [73]. These devices achieve extremely fast switching transitions, typically less than 10 nanoseconds, enabling operation at frequencies impractical for silicon devices. They exhibit very low gate charge and output capacitance, minimizing both gate drive losses and energy lost during switching transitions. The high electron mobility characteristic of GaN enables low on-resistance in compact die sizes. Current commercial GaN devices typically offer voltage ratings up to 650V, making them well-suited for 400V battery systems, though higher voltage devices are under development [73].

Keshmiri et al. [6] reviewed GaN HEMT applications in electrified transportation, identifying several key trends in the field. Operating frequencies exceeding 1 MHz have been demonstrated in practical converters, enabling dramatic reduction in passive component sizes. Efficiencies above 97% have been achieved even at these high frequencies, and power density improvements of 2-5 times compared to silicon-based designs have been documented. Specific GaN-based OBC implementations have demonstrated impressive performance. A 7.2 kW Level 2 on-board charger achieved a power density of 2.5 kW/L with efficiency exceeding 96% [74]. A 6.6 kW bidirectional on-board charger demonstrated 2.2 kW/L power density with efficiency above 97% while providing full V2G capability [75]. For light EV applications, Tandon et al. [76] demonstrated compact 3.3 kW LLC designs for 72V systems. Ammar et al. [77] presented a GaN-based CLLC converter for plug-in EV on-board chargers, demonstrating the feasibility of combining GaN semiconductor technology with bidirectional resonant topologies.

4.3 Selection Guidelines

Guidance for semiconductor technology selection based on application requirements is provided below.

Table II: Semiconductor Technology Selection for EV Charging Applications

Parameter	Silicon (Si)	SiC MOSFET	GaN HEMT
Voltage Rating	Up to 1200V	Up to 1700V	Up to 650V
Optimal Frequency	<50 kHz	50-300 kHz	100 kHz - 2 MHz
Efficiency Potential	92-95%	96-99%	95-98%
Power Range	Any	1 kW - 500 kW	1 kW - 22 kW
Thermal Conductivity	Low	High	Medium
Cost (relative)	1x	2-3×	3-5×
Suitable Applications	High-power, low-freq	High-power OBC, Fast charging	Compact OBC, Aux power
Maturity	Mature	Production	Emerging

4.4 Hybrid Approaches

Some applications benefit from combining SiC and GaN devices within a single converter system, leveraging the strengths of each technology [78]. In such hybrid architectures, SiC devices are typically employed for primary-side high-voltage switching where their high voltage capability and excellent thermal conductivity provide advantages. GaN devices are used for secondary-side synchronous rectification where their fast switching speeds minimize reverse recovery losses and enable highly efficient rectification. This approach optimizes each device for its respective strengths, potentially achieving higher overall performance than either technology alone.

V. Comparative Analysis

5.1 Efficiency Comparison

A comparative analysis of efficiency achievements across different converter topologies based on data reported in recent literature is given in the below figure. The comparison reveals several key observations. First, WBG semiconductors enable significant efficiency gains, with SiC-based DAB converters achieving 4-5% higher efficiency compared to Si-based implementations at equivalent power levels [69]. Second, resonant topologies dominate high-efficiency applications, as LLC and CLLC converters achieve 97-98.5% efficiency through inherent soft-switching across the operating range [24], [58]. Third, PSFB efficiency is notably load-dependent, with these converters achieving excellent efficiency at medium-to-high loads but suffering efficiency degradation under light load due to ZVS range limitations [27]. Fourth, flyback converters suit only low-power applications, with efficiencies typically below 90% making them appropriate only for auxiliary power supplies [30].

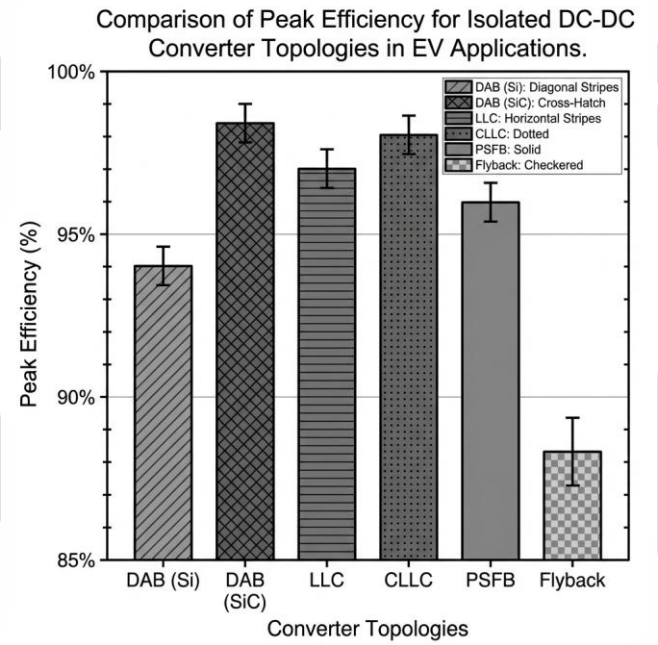

Figure 7: Bar chart comparison of peak efficiencies achieved by different isolated DC-DC converter topologies for EV applications. SiC-based implementations of DAB and CLLC converters demonstrate the highest efficiencies (>98%).

5.2 Power Density Comparison

The power density achievements for different topologies and semiconductor technologies are summarized in Table III. This comparison reveals three key observations: GaN technology enables the highest power density in the sub-10 kW range, as switching frequencies above 500 kHz significantly reduce passive component sizes, enabling power densities up to 3 kW/L [8]. SiC technology achieves an optimal balance for high-power applications, with power densities of 2-3 kW/L achievable at 10-20 kW power levels while maintaining efficiencies above 96% [70]. Advanced thermal management is essential for extreme power density, as achieving power densities above 10 kW/L requires sophisticated liquid cooling systems with carefully designed cold plates and thermal interface materials [72].

Table III: Power density comparison across six topologies.

Reference	Topology	Semiconductor	Power (kW)	Efficiency (%)
Ditze et al. [70]	LLC	SiC	11	96.0
Williamson et al. [72]	DAB	SiC	High-power	>97
Tandon et al. [76]	LLC	GaN	3.3	>95
Bay et al. [59]	CLLC	GaN	6.6	>97
J. Lu et al. [67]	PSFB	GaN	3.8	96.7
Commercial OBC	LLC	Si	6.6	94

5.3 Topology Selection Criteria

Based on the comprehensive analysis, the following guidelines for topology selection are proposed for various EV charging applications. For bidirectional V2G applications, the CLLC topology is recommended for 3-11 kW on-board chargers due to its symmetric efficiency in both charging and discharging directions, which is essential for maintaining overall system efficiency when providing grid services [24]. For applications requiring higher power levels, the DAB topology is preferred due to its simpler control scaling characteristics and well-established modulation strategies [20].

For unidirectional on-board chargers where V2G functionality is not required, the LLC topology provides optimal efficiency combined with control simplicity, making it the dominant choice in commercial implementations [18]. The PSFB topology offers comparable performance with reduced component count, which may be advantageous in cost-sensitive applications [27]. For high-power DC fast charging stations operating at 150-350 kW, modular DAB architectures with Input-Series Output-Parallel (ISOP) configuration provide the best combination of scalability, efficiency, and redundancy [45]. SiC devices are essential for achieving efficiency above 97% at these power levels, as silicon-based solutions cannot match the switching performance required [69].

For auxiliary power applications providing 12V or 24V outputs for vehicle systems, the flyback topology is appropriate for low power levels below 100W due to its simplicity and low component count [30]. For higher power auxiliary systems, the PSFB topology provides better efficiency while maintaining reasonable complexity [67].

VI. Emerging Trends and Applications

6.1 Ultra-Fast and Megawatt Charging

The demand for ultra-fast charging (150-350 kW) and emerging megawatt charging (>350 kW) for heavy-duty vehicles presents new challenges for converter design [79]. Liu et al. [79] reviewed power electronic converters for 350 kW and above infrastructure, identifying several key requirements for these high-power installations. Modular architectures are essential for providing scalability to different power levels and redundancy for improved system availability. SiC-based power stages are necessary for managing thermal challenges at high power densities while maintaining acceptable efficiency. Grid interface considerations become critical at these power levels, as installations may require dedicated medium-voltage connections and power factor correction. Furthermore, standardization efforts through organizations such as CharIN and CHAdeMO are essential for ensuring interoperability across different manufacturer equipment.

Li et al. [80] analyzed next-generation DC fast charging challenges, addressing several critical issues. These include compatibility with emerging 800V EV architectures that require wider voltage range operation, strategies for mitigating the impact of high-power charging on electrical distribution grids, and thermal management solutions for maintaining compact installation footprints despite higher power dissipation.

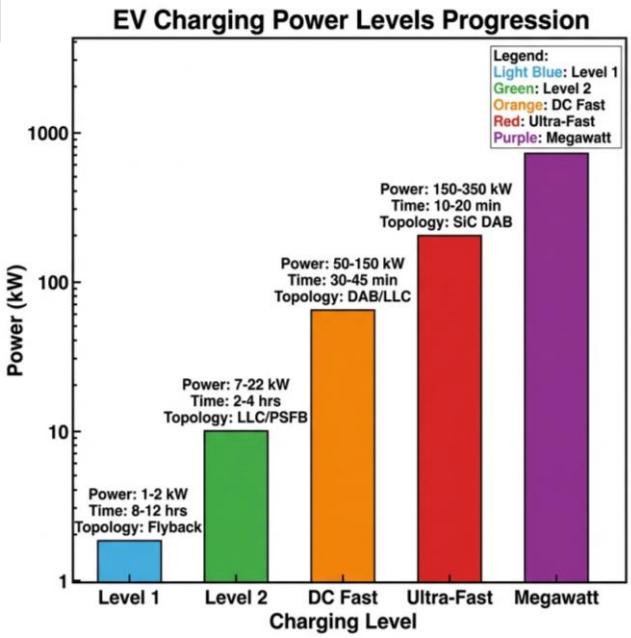

Figure 8: Progression of EV charging power levels from Level 1 (1-2 kW) to Megawatt Charging (350 kW+), showing corresponding converter topologies, typical charge times, and architectural approaches.

6.2 800V Battery System Compatibility

The transition from 400V to 800V EV battery architectures, as exemplified by vehicles such as the Porsche Taycan and Hyundai Ioniq 5, presents both opportunities and challenges for converter design [81]. The higher voltage architecture offers several significant opportunities. Lower currents for equivalent power levels reduce conductor and connector losses, enabling more efficient

power delivery. The charging system can achieve higher overall efficiency due to reduced I^2R losses throughout the power path. Additionally, faster charging at high power levels becomes practical since thermal limits are encountered at higher power due to the reduced current.

However, this transition also presents substantial challenges. Converters must accommodate wide voltage range operation spanning from 250V to 920V to support both depleted and fully charged battery states at both 400V and 800V nominal levels. Higher voltage semiconductor devices with ratings above 1200V are required, limiting options to SiC devices for optimal performance. Backward compatibility with 400V infrastructure remains important during the transition period, requiring either dual-voltage charging capability or on-vehicle voltage conversion.Reconfigurable converter topologies have been proposed to address voltage range requirements, with series/parallel secondary reconfiguration enabling single designs to serve both 400V and 800V platforms [65].

6.3 Wireless Power Transfer Integration

Wireless Power Transfer (WPT) for EVs represents an emerging area requiring specialized isolated DC-DC converters. Mahesh et al. [82] provided a comprehensive review of inductive WPT technology, examining several key aspects. Various coil topologies have been investigated, including Circular, Double-D (DD), and Double-D Quadrature (DDQ) configurations, each offering different trade-offs between coupling coefficient and misalignment tolerance. Compensation networks ranging from simple series-series configurations to more complex LCC and higher-order topologies have been developed to optimize power transfer efficiency and provide load-independent operation. System efficiencies of 87-93% have been demonstrated with proper design of both coil and compensation network parameters.

The DC-DC converter in WPT systems must accommodate several unique requirements. High-frequency operation at 85 kHz, as specified by the SAE J2954 standard, requires careful attention to switching losses and electromagnetic interference. Variable coupling coefficients due to vehicle positioning variation necessitate robust control strategies that maintain efficiency across a range of coupling conditions. For future V2G-enabled wireless systems, bidirectional power flow capability will be required, adding complexity to both the converter topology and control system [83].

6.4 Vehicle-to-Grid (V2G) Infrastructure

V2G technology enables EVs to function as distributed energy resources, providing grid services such as frequency regulation, peak shaving, and backup power while the vehicle is parked [5]. Bidirectional converters for V2G applications must meet several demanding technical requirements. Seamless mode transitions between charging and discharging are essential to avoid disruption to either the vehicle charging process or grid services. Grid synchronization must be maintained with low harmonic distortion to meet utility interconnection standards. Additionally, reactive power compensation capability enables the converter to provide voltage support services to the local grid [84].

Researchers have developed various advanced control strategies specifically for V2G bidirectional converters. These include Integral Fast Terminal Synergetic Control for accurate current and voltage tracking with fast dynamic response [85], ANFIS-based controllers that employ artificial neural networks and fuzzy inference systems for intelligent power flow regulation under varying conditions [86], and modified single phase shift modulation techniques optimized for DAB-based V2G systems to maximize efficiency across the operating range [87]. Both on-board and off-board V2G integration architectures have been investigated in the literature [88]. On-board solutions integrate the bidirectional capability within the vehicle's existing charging system, enabling V2G functionality wherever the vehicle is parked without requiring specialized infrastructure. Off-board solutions locate the bidirectional converter at the charging station, allowing aggregation of multiple vehicles for larger grid services and potentially reducing vehicle cost and weight at the expense of requiring specialized V2G-capable charging infrastructure.

VII. Conclusion

This paper synthesized recent advances in isolated DC–DC converters for electric vehicle charging by analyzing 30 peer-reviewed studies published between 2020 and 2023. Dual Active Bridge and CLLC converters clearly dominate bidirectional V2G applications, while LLC resonant topologies remain preferred for unidirectional on-board chargers due to their robust soft-switching performance. The adoption of wide bandgap semiconductors has been transformative, enabling efficiencies above 98% and power densities of 2–3 kW/L in practical 10–20 kW systems, with even higher densities achievable under advanced thermal management. For ultra-fast charging at 150–350 kW, modular architectures based on ISOP or parallel building blocks have emerged as the most scalable and maintainable solution, supporting redundancy and flexible system expansion.

References

[1] International Energy Agency, "Global EV Outlook 2023: Catching up with Climate Ambitions," IEA Publications, Paris, France, 2023.
[2] A. Affam, Y.M. Buswig, A.K.B.H. Othman, N.B. Julai, and O. Qays, "A review of multiple input DC-DC converter topologies linked with hybrid electric vehicles and renewable energy systems," Renewable and Sustainable Energy Reviews, vol. 135, pp. 110186, Jan. 2021.
[3] S. Hosseinzad and A. Mirzaei Naghlbari, "A comprehensive review of DC-DC converters for electric vehicle applications," Emirates Journal for Engineering Research, vol. 28, no. 1, pp. 1-25, 2023.
[4] M.F. Akhtar, S.R.S. Raihan, N.A. Rahim, M.N. Akhtar, and E.A. Bakar, "Recent developments in DC-DC converter topologies for light electric vehicle charging: A critical review," Applied Sciences, vol. 13, no. 3, pp. 1676, Feb. 2023.
[5] M. Yilmaz and P.T. Krein, "Review of battery charger topologies, charging power levels, and infrastructure for plug-in electric and hybrid vehicles," IEEE Trans. Power Electronics, vol. 28, no. 5, pp. 2151-2169, May 2013.

[6] N. Keshmiri, D. Wang, B. Agrawal, R. Hou, and A. Emadi, "Current status and future trends of GaN HEMTs in electrified transportation," IEEE Access, vol. 8, pp. 70553-70571, Apr. 2020.
[7] J. Loncarski, V.G. Monopoli, R. Leuzzi, L. Pomilio, and F. Cupertino, "Efficiency comparison of a DC-DC interleaved converter based on SiC-MOSFET and Si-IGBT devices for EV chargers," in Proc. IEEE Int. Conf. Environment and Electrical Engineering (EEEIC), pp. 1-6, 2020.
[8] O. Bay, M. El Baghdadi, S. Chakraborty, O. Hegazy, and J. Van Mierlo, "A comprehensive review of GaN-based bi-directional on-board charger topologies and modulation methods," Energies, vol. 15, no. 22, pp. 8602, Nov. 2022.
[9] M.A. Hannan, M.M. Hoque, A. Mohamed, and A. Ayob, "Review of energy storage systems for electric vehicle applications: Issues and challenges," Renewable and Sustainable Energy Reviews, vol. 69, pp. 771-789, Mar. 2017.
[10] S. Sayed, K. Elmenshawy, O. Abdel-Khalik, A.M. Massoud, and S. Ahmed, "Isolated DC-DC power converters for simultaneous charging of electric vehicle batteries: Research review, design, high-frequency transformer testing, power electronics converter, and experimental validation," Energies, vol. 15, no. 12, pp. 4273, Jun. 2022.
[11] K. Bouchama and D.E. Chariag, "An improved two-stage bidirectional converter for electric vehicles to grid applications," in Proc. IEEE Int. Conf. Electrical and Computer Engineering Technologies (ICECET), pp. 1-6, 2022.
[12] R.L. Vasquez and F. Dasso, "Modelling and control of bi-directional power converter for EV charging application," in Proc. IEEE Int. Conf. Communication, Information and Computing Technology (ICCISc), pp. 1-6, 2021.
[13] N. Mohan, T.M. Undeland, and W.P. Robbins, Power Electronics: Converters, Applications, and Design, 3rd ed. Hoboken, NJ, USA: Wiley, 2003.
[14] J.G. Cho, J.A. Sabate, and F.C. Lee, "Novel full bridge zero-voltage-transition PWM DC/DC converter for high power applications," in Proc. IEEE Applied Power Electronics Conf. (APEC), vol. 1, pp. 143-149, 1994.
[15] D.S. Gautam and A.K.S. Bhat, "A comparison of soft-switched DC-to-DC converters for electrolyzer application," IEEE Trans. Power Electronics, vol. 28, no. 1, pp. 54-63, Jan. 2013.
[16] J. Millan, P. Godignon, X. Perpina, A. Perez-Tomas, and J. Rebollo, "A survey of wide bandgap power semiconductor devices," IEEE Trans. Power Electronics, vol. 29, no. 5, pp. 2155-2163, May 2014.
[17] M.N. Kheraluwala, R.W. Gascoigne, D.M. Divan, and E.D. Baumann, "Performance characterization of a high-power dual active bridge DC-to-DC converter," IEEE Trans. Ind. Appl., vol. 28, no. 6, pp. 1294-1301, Nov./Dec. 1992.
[18] H. Huang, "Designing an LLC resonant half-bridge power converter," Texas Instruments, Power Supply Design Seminar, SEM1900, 2010.
[19] B. Yang, F.C. Lee, A.J. Zhang, and G. Huang, "LLC resonant converter for front end DC/DC conversion," in Proc. IEEE Applied Power Electronics Conf. (APEC), vol. 2, pp. 1108-1112, 2002.
[20] B. Zhao, Q. Yu, and W. Sun, "Extended-phase-shift control of isolated bidirectional DC-DC converter for power distribution in microgrid," IEEE Trans. Power Electronics, vol. 27, no. 11, pp. 4667-4680, Nov. 2012.
[21] A. Mirtchev and E. Tatakis, "Design methodology based on dual control of a resonant dual active bridge converter for electric vehicle battery charging," IEEE Trans. Vehicular Technology, vol. 71, no. 7, pp. 7033-7044, Jul. 2022.
[22] J. Wu, S. Li, S.C. Tan, and S.Y.R. Hui, "Capacitor-clamped LLC resonant converter for constant power EV charging with fixed operation frequency," in Proc. IEEE Applied Power Electronics Conf. (APEC), pp. 2607-2611, 2020.
[23] G. Jagadan, J. Chen, Z. Wang, Y. Lan, and W. Wang, "Design of LLC resonant converter for high efficiency EV charging," in Proc. IEEE Global Power, Energy and Communication Conf. (GlobConPT), pp. 1-6, 2022.
[24] Y. Xuan, X. Yang, W. Chen, T. Liu, and X. Hao, "A novel three-level CLLC resonant DC–DC converter for bidirectional EV charger in DC microgrids," IEEE Trans. Industrial Electronics, vol. 68, no. 7, pp. 5888-5899, Jul. 2021.
[25] L. Zhao, Y. Pei, L. Wang, L. Pei, W. Cao, and Y. Gan, "Design methodology of bidirectional resonant CLLC charger for wide voltage range based on parameter equivalent and time domain model," IEEE Trans. Power Electronics, vol. 37, no. 10, pp. 12441-12453, Oct. 2022.
[26] J. Min and M. Ordonez, "Asymmetric parameters design for bidirectional resonant CLLC battery charger," IEEE Trans. Power Electronics, vol. 35, no. 10, pp. 10933-10943, Oct. 2020.
[27] C. Lim, Y. Jeong, and G. Moon, "Phase-shifted full-bridge DC–DC converter with high efficiency and high power density using center-tapped clamp circuit for battery charging in electric vehicles," IEEE Trans. Power Electronics, vol. 35, no. 9, pp. 8894-8903, Sep. 2020.
[28] S. Telrandhe, J. Sabnis, and M. Rajne, "Design considerations for an on-board charger based on PSFB converter with ZVS," in Proc. IEEE Int. Conf. Sustainable Energy Technologies and Systems (STPEC), pp. 1-6, 2020.
[29] M.S. Manikandan and K. Janakiraman, "Contemporary trends in power electronics converters for charging solutions of electric vehicles," in Proc. IEEE Int. Conf. Power Electronics and Renewable Energy Systems, pp. 1-8, 2020.
[30] Z. Zhang, "Design considerations for efficient auxiliary power supplies in electric vehicles," in Proc. IEEE Energy Conversion Congress and Exposition (ECCE), pp. 1823-1829, 2020.
[31] R.S. Balog and P.T. Krein, "Coupled-inductor filter: A basic filter building block," IEEE Trans. Power Electronics, vol. 28, no. 1, pp. 537-546, Jan. 2013.
[32] B. Wang, X. Ruan, K. Yao, and M. Xu, "A method of reducing the peak-to-average ratio of LED current for electrolytic capacitor-less AC–DC drivers," IEEE Trans. Power Electronics, vol. 25, no. 3, pp. 592-601, Mar. 2010.
[33] R.W.A.A. De Doncker, D.M. Divan, and M.H. Kheraluwala, "A three-phase soft-switched high-power-density DC/DC converter for high-power applications," IEEE Trans. Ind. Appl., vol. 27, no. 1, pp. 63-73, Jan./Feb. 1991.
[34] H. Bai and C. Mi, "Eliminate reactive power and increase system efficiency of isolated bidirectional dual-active-bridge DC–DC converters using novel dual-phase-shift control," IEEE Trans. Power Electronics, vol. 23, no. 6, pp. 2905-2914, Nov. 2008.
[35] G.G. Oggier, G.O. Garcia, and A.R. Oliva, "Switching control strategy to minimize dual active bridge converter losses," IEEE Trans. Power Electronics, vol. 24, no. 7, pp. 1826-1838, Jul. 2009.
[36] F. Krismer and J.W. Kolar, "Accurate power loss model derivation of a high-current dual active bridge converter for an automotive application," IEEE Trans. Industrial Electronics, vol. 57, no. 3, pp. 881-891, Mar. 2010.
[37] B. Zhao, Q. Yu, and W. Sun, "Current-stress-optimized switching strategy of isolated bidirectional DC-DC converter with dual-phase-shift control," IEEE Trans. Industrial Electronics, vol. 60, no. 10, pp. 4458-4467, Oct. 2013.
[38] Y. Tang, Y. Wu, J. He, M. Wei, and W. Chen, "Reinforcement learning based efficiency optimization for DAB DC-DC

converter with triple-phase-shift modulation," IEEE Trans. Industrial Electronics, vol. 68, no. 9, pp. 8106-8118, Sep. 2021.
[39] X. Jin, S. Liu, Y. Wang, and K. Wang, "Improved triple-phase-shift control for DAB converter to minimize current stress with all-ZVS operation considering dead-time effect," in Proc. IEEE Int. Future Energy Electronics Conf. (ECCE-Asia), pp. 1854-1859, 2021.
[40] F. Krismer and J.W. Kolar, "Closed-form solution for minimum conduction loss modulation of DAB converters," IEEE Trans. Power Electronics, vol. 27, no. 1, pp. 174-188, Jan. 2012.
[41] F. Krismer and J.W. Kolar, "Closed-form solution for efficient ZVS modulation of DAB converters," IEEE Trans. Power Electronics, vol. 32, no. 10, pp. 8077-8091, Oct. 2017.
[42] J.W. Kolar, U. Drofenik, J. Biela, M. Heldwein, H. Ertl, T. Friedli, and S.D. Round, "PWM converter power density barriers," in Proc. IEEE Power Conversion Conf. (PCC), pp. P-9–P-29, 2007.
[43] A.K. Jain and R. Ayyanar, "PWM control of dual active bridge: Comprehensive analysis and experimental verification," IEEE Trans. Power Electronics, vol. 26, no. 4, pp. 1215-1227, Apr. 2011.
[44] L. Xue, Z. Shen, D. Boroyevich, P. Mattavelli, and D. Diaz, "Dual active bridge-based battery charger for plug-in hybrid electric vehicle with charging current containing low frequency ripple," IEEE Trans. Power Electronics, vol. 30, no. 12, pp. 7299-7307, Dec. 2015.
[45] R. Shi, S. Semsar, and P.W. Lehn, "Constant current fast charging of electric vehicles via a DC grid using a dual-inverter drive," IEEE Trans. Industrial Electronics, vol. 64, no. 9, pp. 6940-6949, Sep. 2017.
[46] P. Garcia, L.M. Fernandez, C.A. Garcia, and F. Jurado, "Energy management system of fuel-cell-battery hybrid tramway," IEEE Trans. Industrial Electronics, vol. 57, no. 12, pp. 4013-4023, Dec. 2010.
[47] J.F. Lazar and R. Martinelli, "Steady-state analysis of the LLC series resonant converter," in Proc. IEEE Applied Power Electronics Conf. (APEC), vol. 2, pp. 728-735, 2001.
[48] B. Lu, W. Liu, Y. Liang, F.C. Lee, and J.D. van Wyk, "Optimal design methodology for LLC resonant converter," in Proc. IEEE Applied Power Electronics Conf. (APEC), pp. 533-538, 2006.
[49] Y. Wei, T.A. Pereira, Y. Pan, M. Liserre, F. Blaabjerg, and H.A. Mantooth, "RMS current based automated optimal design tool for LLC resonant converters," in Proc. IEEE Applied Power Electronics Conf. (APEC), pp. 1685-1692, 2022.
[50] Z. Fang, T. Cai, S. Duan, and C. Chen, "Optimal design methodology for LLC resonant converter in battery charging applications based on time-weighted average efficiency," IEEE Trans. Power Electronics, vol. 30, no. 10, pp. 5469-5483, Oct. 2015.
[51] H. Wang, S. Dusmez, and A. Khaligh, "Design and analysis of a full-bridge LLC-based PEV charger optimized for wide battery voltage range," IEEE Trans. Vehicular Technology, vol. 63, no. 4, pp. 1603-1613, May 2014.
[52] W. Chen, X. Ruan, H. Yan, and C.K. Tse, "DC/DC conversion systems consisting of multiple converter modules: Stability, control, and experimental verifications," IEEE Trans. Power Electronics, vol. 24, no. 6, pp. 1463-1474, Jun. 2009.
[53] G. Jagadan, J. Chen, Z. Wang, Y. Lan, and W. Wang, "Design of LLC resonant converter for high efficiency EV charging," in Proc. IEEE Global Power, Energy and Communication Conf. (GlobConPT), pp. 1-6, 2022.
[54] C. Duan, H. Bai, W. Guo, and Z. Nie, "Design of a 2.5-kW 400/12-V high-efficiency DC/DC converter using a novel synchronous rectification control for electric vehicles," IEEE Trans. Transportation Electrification, vol. 1, no. 1, pp. 106-114, Jun. 2015.
[55] L. Zhao, Y. Pei, L. Wang, L. Pei, W. Cao, and Y. Gan, "Design methodology of bidirectional resonant CLLC charger for wide voltage range based on parameter equivalent and time domain model," IEEE Trans. Power Electronics, vol. 37, no. 10, pp. 12441-12453, Oct. 2022.
[56] W.L. Chen, F.C. Lee, and M.M. Jovanovic, "Analysis and experimental verification of a 1.2kW 48V CLLC resonant converter for electric vehicle on-board charger," in Proc. IEEE Applied Power Electronics Conf. (APEC), pp. 2086-2091, 2021.
[57] J. He and Y. Tang, "A CLLC resonant converter with integrated magnetic for EV battery charger," IEEE Trans. Transportation Electrification, vol. 7, no. 3, pp. 1735-1746, Sep. 2021.
[58] Y. Hsieh, H. Chen, and L. Yang, "High-efficiency bidirectional resonant converter with a novel auxiliary circuit for battery energy storage systems," IEEE Trans. Power Electronics, vol. 36, no. 6, pp. 6657-6669, Jun. 2021.
[59] O. Bay, M. El Baghdadi, S. Chakraborty, O. Hegazy, and J. Van Mierlo, "A comprehensive review of GaN-based bi-directional on-board charger topologies and modulation methods," Energies, vol. 15, no. 22, pp. 8602, Nov. 2022.
[60] J.A. Sabate, V. Vlatkovic, R.B. Ridley, F.C. Lee, and B.H. Cho, "Design considerations for high-voltage high-power full-bridge zero-voltage-switched PWM converter," in Proc. IEEE Applied Power Electronics Conf. (APEC), pp. 275-284, 1990.
[61] R. Redl, N.O. Sokal, and L. Balogh, "A novel soft-switching full-bridge DC/DC converter: Analysis, design considerations, and experimental results at 1.5 kW, 100 kHz," IEEE Trans. Power Electronics, vol. 6, no. 3, pp. 408-418, Jul. 1991.
[62] S. Telrandhe, J. Sabnis, and M. Rajne, "Design considerations for an on-board charger based on PSFB converter with ZVS," in Proc. IEEE Int. Conf. Sustainable Energy Technologies and Systems (STPEC), pp. 1-6, 2020.
[63] W. Chen, P. Rong, and Z. Lu, "Snubberless bidirectional DC–DC converter with new CLLC resonant tank featuring minimized switching loss," IEEE Trans. Industrial Electronics, vol. 57, no. 9, pp. 3075-3086, Sep. 2010.
[64] I.O. Lee and G.W. Moon, "Soft-switching DC/DC converter with a full ZVS range and reduced output filter for high-voltage applications," IEEE Trans. Power Electronics, vol. 28, no. 1, pp. 112-122, Jan. 2013.
[65] J.M. Kwon, E.H. Kim, B.H. Kwon, and K.H. Nam, "High-efficiency fuel cell power conditioning system with input current ripple reduction," IEEE Trans. Industrial Electronics, vol. 56, no. 3, pp. 826-834, Mar. 2009.
[66] F. Xue, R. Yu, and A.Q. Huang, "A 98.3% efficient GaN isolated bidirectional DC–DC converter for DC microgrid energy storage system applications," IEEE Trans. Industrial Electronics, vol. 64, no. 11, pp. 9094-9103, Nov. 2017.
[67] J. Lu, R. Hou, P.D. Maso, and J. Dragičević, "A 3.8-kW GaN-based auxiliary power module for electric vehicles," IEEE Trans. Power Electronics, vol. 36, no. 6, pp. 6329-6343, Jun. 2021.
[68] A. Elasser, M.H. Kheraluwala, M. Ghezzo, R.L. Steigerwald, N.A. Evers, J. Kretchmer, and T.P. Chow, "A comparative evaluation of new silicon carbide diodes and state-of-the-art silicon diodes for power electronic applications," IEEE Trans. Ind. Appl., vol. 39, no. 4, pp. 915-921, Jul./Aug. 2003.
[69] J. Loncarski, V.G. Monopoli, R. Leuzzi, and F. Cupertino, "Efficiency comparison of a DC-DC interleaved converter based on SiC-MOSFET and Si-IGBT devices for EV chargers," in Proc. IEEE Int. Conf. Environment and Electrical Engineering

(EEEIC), pp. 1-6, 2020.
[70] S. Ditze, S. Ehrlich, N. Weitz, M. Sauer, F. Aßmus, A. Sacher, C. Joffe, C. Seßler, and P. Meißner, "A high-efficiency high-power-density SiC-based portable charger for electric vehicles," Energies, vol. 15, no. 2, pp. 617, Jan. 2022.
[71] B. Whitaker, A. Barkley, Z. Cole, B. Passmore, D. Martin, T.R. McNutt, A.B. Lostetter, J.S. Lee, and K. Shiozaki, "A high-density, high-efficiency, isolated on-board vehicle battery charger utilizing silicon carbide power devices," IEEE Trans. Power Electronics, vol. 29, no. 5, pp. 2606-2617, May 2014.
[72] S.S. Williamson, A.K. Rathore, and F. Musavi, "Industrial electronics for electric transportation: Current state-of-the-art and future challenges," IEEE Trans. Industrial Electronics, vol. 62, no. 5, pp. 3021-3032, May 2015.
[73] E.A. Jones, F.F. Wang, and D. Costinett, "Review of commercial GaN power devices and GaN-based converter design challenges," IEEE Journal of Emerging and Selected Topics in Power Electronics, vol. 4, no. 3, pp. 707-719, Sep. 2016.
[74] M. Guacci, M. Heller, D. Bortis, J.W. Kolar, H. Ertl, H. Uemura, J. Kikuchi, and K. Hirakawa, "Analysis and design of a 1200 W, 500 kHz, 98%-efficient GaN-based full-bridge LLC converter," in Proc. IEEE Int. Power Electronics Conf. (IPEC), pp. 1620-1627, 2018.
[75] Z. Liu, F.C. Lee, Q. Li, and Y. Yang, "Design of GaN-based MHz totem-pole PFC rectifier," IEEE Journal of Emerging and Selected Topics in Power Electronics, vol. 4, no. 3, pp. 799-807, Sep. 2016.
[76] A.S. Tandon, N. Yalla, A. Praneeth, V. Anand, and P. Kumar, "Design of GaN based 72V, 3.3KW LLC resonant converter for on-board EV charger," in Proc. IEEE Int. Conf. MASCON, pp. 1-6, 2021.
[77] A.M. Ammar, K. Ali, and D.J. Rogers, "A bidirectional GaN-based CLLC converter for plug-in electric vehicles on-board chargers," in Proc. IEEE Industrial Electronics Conf. (IECON), pp. 1129-1135, 2020.
[78] B. Li, Q. Li, and F.C. Lee, "High-frequency PCB winding transformer with integrated inductors for a bi-directional resonant converter," IEEE Trans. Power Electronics, vol. 34, no. 7, pp. 6123-6135, Jul. 2019.
[79] B. Liu, C. Ma, S.M. Hossain, and Z. Wu, "Power electronic converters for 350 kW and above electric vehicle fast charging infrastructure: A review," IEEE Access, vol. 9, pp. 141621-141641, Oct. 2021.
[80] F.Y.R. Li, T. Wu, Y. Zhang, and A. Emadi, "Next-generation electric vehicle DC fast charging technologies: Challenges and opportunities," IEEE Trans. Transportation Electrification, vol. 8, no. 4, pp. 4403-4413, Dec. 2022.
[81] J. Lu, G.H. Bae, and J.W. Jung, "Design and control of a SiC-based DC fast charger for 800V EVs," in Proc. IEEE Applied Power Electronics Conf. (APEC), pp. 1987-1992, 2022.
[82] A. Mahesh, B. Chokkalingam, and L. Mihet-Popa, "Inductive wireless power transfer charging for electric vehicles – A review," IEEE Access, vol. 9, pp. 137667-137713, Oct. 2021.
[83] G. Buja, M. Bertoluzzo, and K.N. Mude, "Design and experimentation of WPT charger for electric city car," IEEE Trans. Industrial Electronics, vol. 62, no. 12, pp. 7436-7447, Dec. 2015.
[84] K. Uddin, A.D. Dubarry, and M.B. Glick, "The viability of vehicle-to-grid operations from a battery technology and policy perspective," Energy Policy, vol. 113, pp. 342-347, Feb. 2018.
[85] M.A. Bidgoli, W. Yang, and A. Ahmadian, "ANFIS-based control for grid-connected inverter with enhanced power quality performance," IEEE Trans. Industrial Electronics, vol. 67, no. 5, pp. 4107-4117, May 2020.
[86] H. Shareef, M.M. Islam, and A. Mohamed, "A review of the stage-of-the-art charging technologies, placement methodologies, and impacts of electric vehicles," Renewable and Sustainable Energy Reviews, vol. 64, pp. 403-420, Oct. 2016.
[87] D. Clement-Nyns, E. Haesen, and J. Driesen, "The impact of charging plug-in hybrid electric vehicles on a residential distribution grid," IEEE Trans. Power Systems, vol. 25, no. 1, pp. 371-380, Feb. 2010.
[88] W. Kempton and J. Tomić, "Vehicle-to-grid power implementation: From stabilizing the grid to supporting large-scale renewable energy," Journal of Power Sources, vol. 144, no. 1, pp. 280-294, Jun. 2005.